

Synthesis and electrical and opto-electronic properties of poly(*N*-ethyl carbazolyle)methane

Panchanan Pramanik* and Md. Aquil Akhter

Department of Chemistry, Indian Institute of Technology, Kharagpur 721302, India

(Received 6 October 1986; revised 8 September 1987; accepted 15 October 1987)

Poly(*N*-ethyl carbazolyle)methane was synthesized by the condensation polymerization of *N*-ethylcarbazole and formalin (30% HCHO in water) and studied for electrical and opto-electronic properties. Both dark and photoconductivity of the polymer film were investigated by steady-state measurements. Current-voltage characteristics and intrinsic photoconduction of the polymer in the visible wavelength range were studied. The current increases superlinearly which has been tentatively explained by the Poole-Frenkel effect. Dielectric constant and dielectric loss parameters of the polymer were measured over a frequency range of 50 Hz–10 kHz and a temperature range of 300–344 K. The growth and decay rate of the photocurrent depends on the applied voltage, and the photocurrent directly varies with intensity of light. The activation energies for dark and photoconductivity are 0.34 and 0.3 eV, respectively, and the spectral dependence of the photocurrent produced maxima at 2.75 eV.

(Keywords: poly(*N*-ethyl carbazolyle)methane; conductivity; activation energy; space charge limited current; Poole-Frenkel effect; absorption coefficient; trapped carriers; thermally stimulated current)

INTRODUCTION

In the course of our investigation^{1,2} on the synthesis and evaluation of photoconducting polymers we became interested in a polycondensate poly(*N*-ethyl carbazolyle)methane (PNECM). Photoconductivity is a very useful variable in the study of the conduction mechanism and the electronic structure of polymers. The trap centre is assigned to the defect caused mostly by oxidized quinonoid type of species which is equivalent to different lengths of unsaturated bond cavities in the amorphous³⁻⁶ or carbonyl group^{3,7} by the use of thermally stimulated current (t.s.c.). In view of the paucity of any relevant information on the electrical, opto-electronic and t.s.c. of PNECM, we have examined these properties of the polymer in detail.

EXPERIMENTAL

Synthesis of the polymer

The polymer PNECM was prepared by the condensation polymerization method in nitrogen atmosphere. Commercial grade *N*-ethylcarbazole (manufactured by Fluka AG) was recrystallized repeatedly from chloroform; m.p. 67.5°C, n.m.r. (CDCl₃) δ : 1.3–1.45 (t, 3H), 4.15–4.45 (q, 2H), 7.1–8.1 (m, 8H) ppm. *N*-ethylcarbazole, 1.952 g dissolved in 6M HCl (10 ml) was treated with 30% formalin (1.0 ml) at 80°C for 9 h. The polymer was obtained as a light brown material on cooling. The viscous precipitate was washed with hot MeOH and reprecipitated from CHCl₃-MeOH and dried in a vacuum desiccator. The structure shown in Figure 1 of PNECM was confirmed by elemental analysis and n.m.r. (CDCl₃) δ : 1.1–1.5 (m, 3H), 4.15–4.55 (m, 4H), 7–8.18 (m, 6H) ppm. All the n.m.r. spectra were recorded

on a 90 MHz varian n.m.r. instrument using TMS as internal standard.

Molecular weight

The average molecular weight of PNECM, as measured by Knauer vapour pressure osmometry in chloroform solution, was found to be 13 000.

Thermogravimetry

Thermal analysis in the atmosphere was carried out with a MOM derivatograph, Paulik-Paulik, Hungary (Model no. 874373), up to a temperature of 900°C with Al₂O₃ as the standard, and a linear heating rate of 10°C min⁻¹ and sensitivity of thermogravimetric analysis (t.g.a.) = 1/10 and $T_g = 200^\circ\text{C}$.

X-ray diffraction

This was obtained using a Jeol, Japan (Model: JDX-8P) unit with FeK α radiation, and indicated the amorphous nature of PNECM.

Preparation of film

Figure 2 illustrates the procedure² followed. A piece of Teflon-shielded wire was pasted onto a tiny area by silver paint on the top surface of the conducting SnO₂ Nesa glass plate (2 × 2.5 cm²). This small area was covered with a dilute solution of PNECM in THF and the solvent was

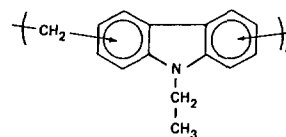


Figure 1 Structure of poly(*N*-ethyl carbazolyle)methane

* To whom correspondence should be addressed

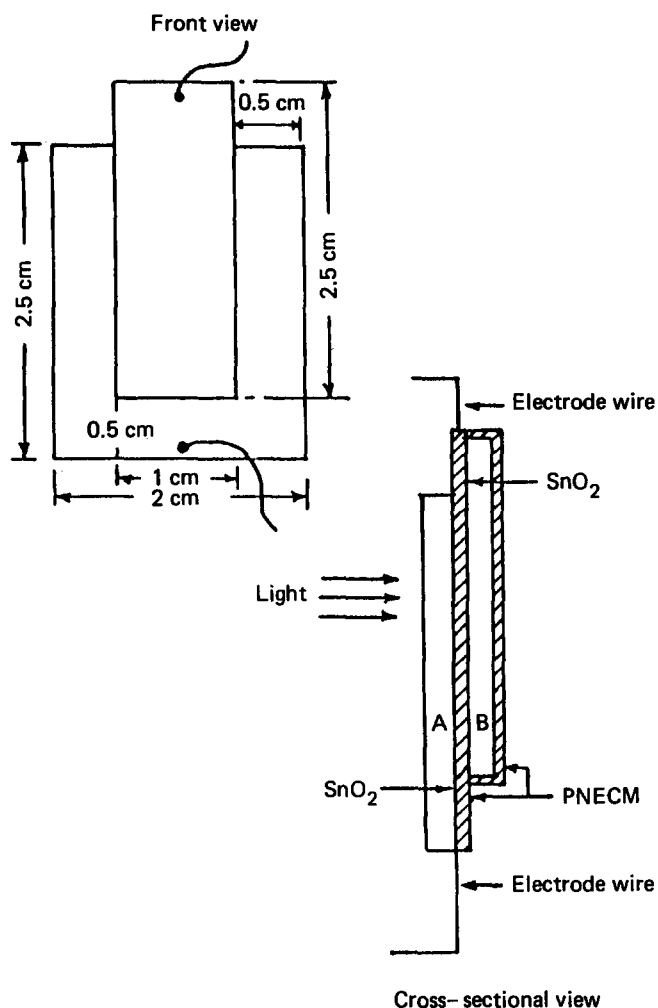


Figure 2 Sandwiched film configuration of the type $\text{SnO}_2/\text{PNECM}/\text{SnO}_2$

allowed to evaporate. The same procedure was followed to fix another electrode wire on a smaller conducting SnO_2 Nesa glass plate ($1 \times 2.5 \text{ cm}^2$). A dilute solution of PNECM in THF was poured on the large conducting glass plate with the electrode wire, and THF was allowed to evaporate slowly in a chamber with a narrow outlet containing a small amount of THF. The other smaller conducting glass plate with electrode wire was immersed completely in a very dilute solution of PNECM, and then taken out of the solution and allowed to evaporate in the THF chamber. The conducting glass plate now coated with the sticky polymer layer was then pressed on the previously prepared film. The assembly (Figure 2) was finally dried in a vacuum desiccator. The film thickness was found to be $31.5\text{--}32.8 \mu\text{m}$ by weighing⁸. Thus, Teflon-shielded anchoring of the lead in wire at two points covered fully with PNECM served as a two electrode wire connection, and also prevented the surface current flow. In this manner, the film samples were always in a sandwiched configuration^{2,8} of the type $\text{SnO}_2/\text{PNECM}/\text{SnO}_2$. The surface current flow was checked with this type of configuration on PVC and polystyrene polymers, and the values obtained were compared with those from conventional methods.

Dark and photoconductivity

The steady-state measurements of PNECM film (thickness $32 \mu\text{m}$ and density 0.78 g cm^{-3}) were

performed in a dark vacuum chamber provided with electrostatic shielding, a sample holder, a window and shielded electrical leads for mounting the sample. The experimental circuit arrangements^{2,8} were made for dark and photocurrent measurements under vacuum (10^{-5} Torr) with a white light source (tungsten-halogen lamp 600 W, 230 V) by standard technique using stabilized d.c. power supply (CEL) and Keithly electrometer (610C, USA). The growth and decay characteristics were traced on a X-Y recorder coupled to the electrometer. The intensity variation characteristics were investigated by changing the source-to-sample distance, and the actual value of intensity falling on the sample was measured using a radiometer (CEL SM204). The spectral response was measured by the following procedure. Light from the tungsten-halogen lamp after passing through the monochromator (CEL, HM 104) illuminated the sample. The photocurrent and photon number were measured for different wavelengths by means of an electrometer and photon counter (CEL) from which the normalized graph was obtained. The intensity of each wavelength was calibrated with a radiometer. However, for minimizing any thermal effect due to infrared radiation, the light was filtered throughout the experiment by means of a water-i.r. filter (thickness 2 cm and diameter 3 cm) surrounded by a glass spiral through which cooling water was flowing.

Visible absorption spectra

Absorption spectra of PNECM film was measured with a Carry 17-D spectrophotometer.

Dielectric constant and dielectric loss

The dielectric constant and dielectric loss were measured in the frequency range (50 Hz–10 kHz) and temperature range 300–344 K) by means of a capacitance bridge (GR-1620 AP, USA).

Thermally stimulated current

The experimental procedure⁶ is as follows. The t.s.c. measurement was carried out in vacuum (10^{-5} Torr). The sample (thickness $32 \mu\text{m}$ in a sandwiched configuration) is cooled to a low temperature and irradiated with a tungsten-halogen lamp (600 W) for 30 min so that traps are filled with carriers. Then the bias voltage of 150 V is applied. After the transient current is reduced to a negligible small value, the sample temperature is slowly increased at the rate of 5°C min^{-1} from low temperature to a high temperature near the softening point of the sample. A t.s.c. spectrum is recorded by a recorder connected to the electrometer. The bias voltage is removed from the sample at near the softening point, and the sample is recooled to a low temperature and reheated at the same rate after application of the same bias voltage. The second cycle spectrum is recorded connected to an electrometer.

RESULTS AND DISCUSSION

The structure of the polymer shown in Figure 1 was freely soluble in chloroform and THF.

Thermogravimetry

The results of t.g.a. and differential thermal analysis (d.t.a.) are presented in Figure 3. The softening

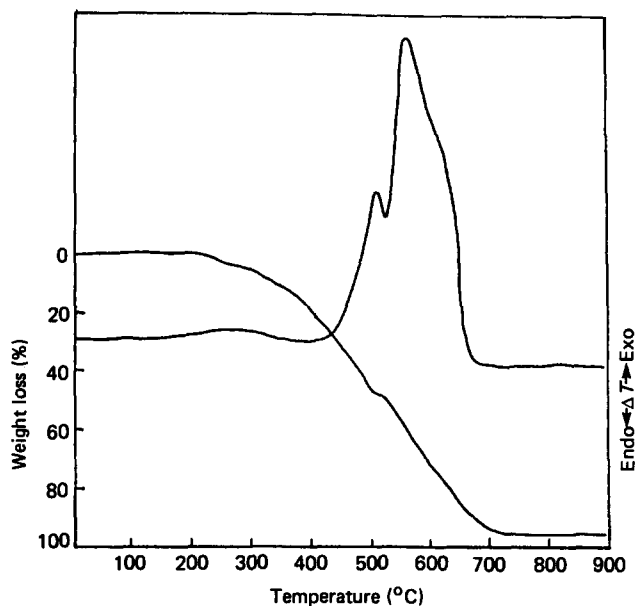


Figure 3 Thermogravimetric analysis of PNECM

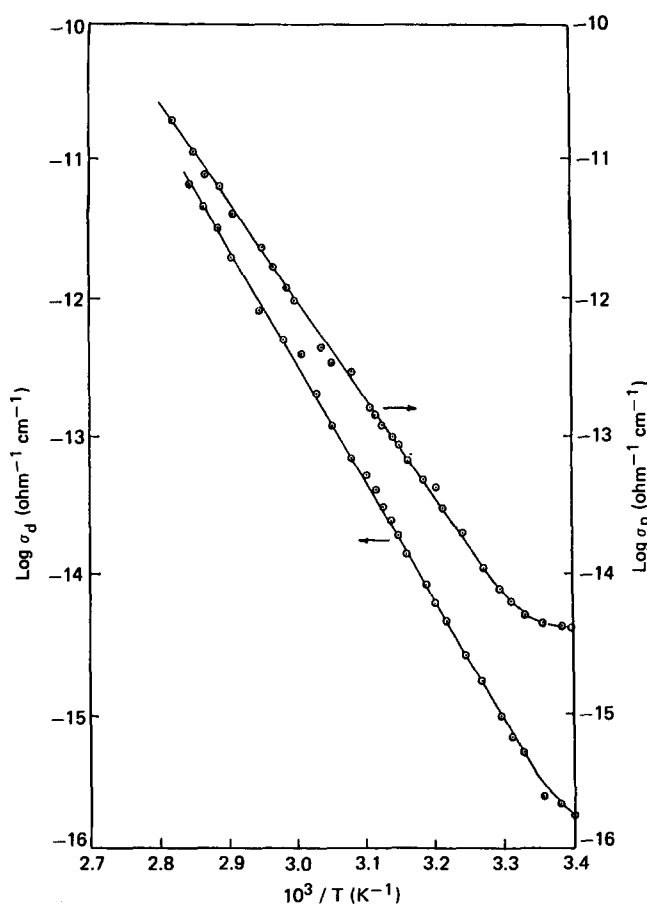


Figure 4 Dark and photoconductivity variation with temperature of PNECM film (intensity of illumination for photoconductivity = 120 mW cm⁻²)

temperature of PNECM is 89°C. The presence of two sharp exothermic peaks at 510 and 556°C are due to the oxidative degradation of PNECM.

Dark and photoconductivity

The dark conductivity (σ_d) of PNECM film at room temperature is found to be $10^{-16} \Omega^{-1} \text{ cm}^{-1}$ which is

comparable to that of poly(methyl pentene)⁹ and poly(*N*-benzylidiphenylamino)methane². The majority carrier appears to be electrons by the thermal probe method. The temperature dependence of dark conductivity (σ_d) and photoconductivity (σ_p) of a typical PNECM film are shown in Figure 4. The dark conductivity and photoconductivity both are thermally activated with activation energies of 0.34 and 0.30 eV, respectively.

Current-voltage characteristics

The dark current-voltage characteristics of PNECM film are shown in Figure 5 at different temperature. It is seen that up to 200 V the plots are ohmic, after which the curves are superlinear. The superlinearity indicates that the current transport is space charge limited⁹. Above 200 V the graph represents the shallow trap¹⁰, while above 600 V the trap-filled limit^{11,12} occurs.

The non-linear space charge limited current (SCLC)-voltage characteristics at high voltage region represents the Poole-Frenkel (PF) effect. The PF effect refers to an electric field-assisted thermal ionization of the negative carriers from the coulombic well, i.e. charge potential well usually associated with a positive charge trap. There is no PF effect if the traps are uncharged when empty. Figure 6 shows the PF plot^{9,13} (semi-log plot of current density vs. $F^{1/2}$) of the same dark current-voltage characteristics. From the slope of this curve, the PF constant was evaluated as shown in Table 1. The value calculated from the field dependence of conductivity¹³ corresponds to that of polyvinylcarbazole¹⁴.

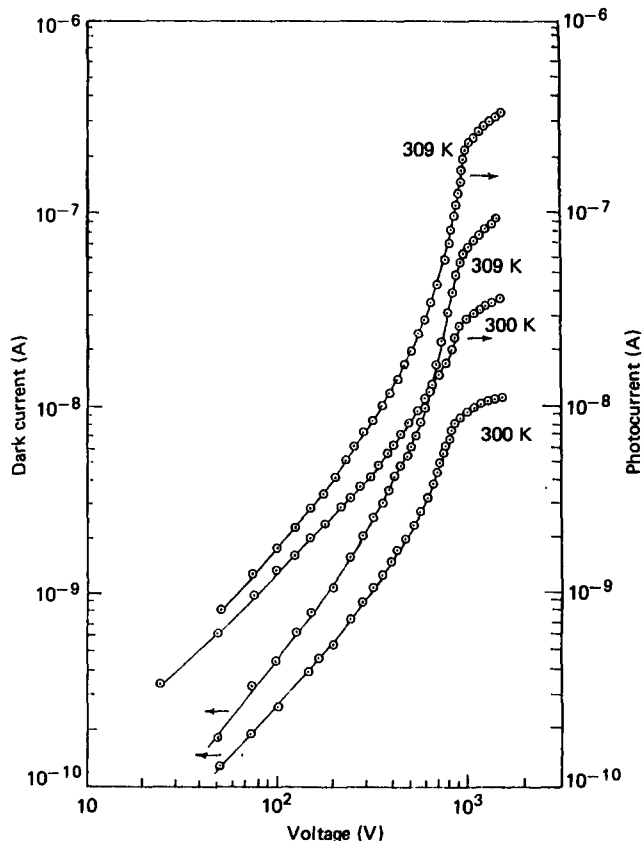


Figure 5 Current-voltage characteristics of PNECM film at two different temperatures

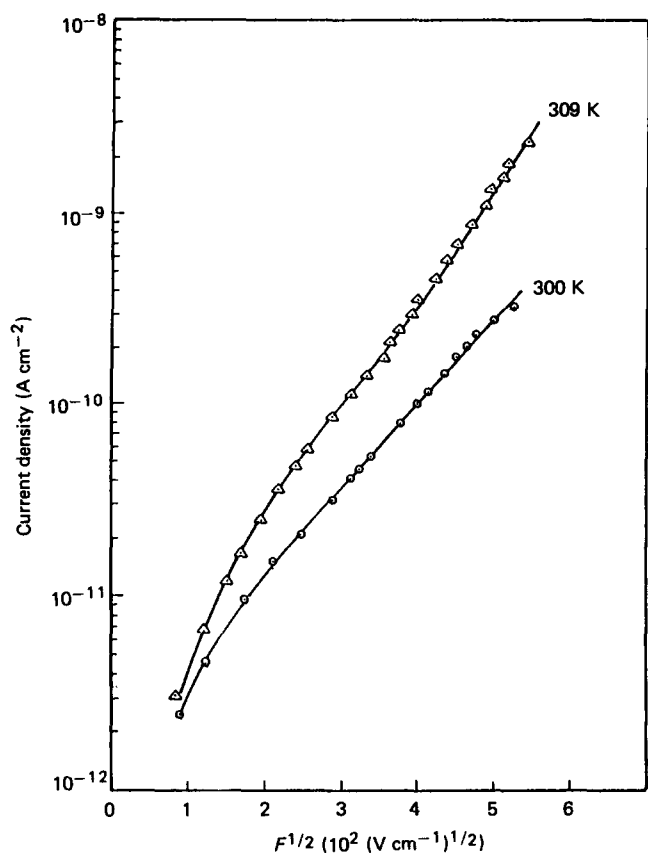


Figure 6 Poole-Frenkel plots (semi-log plot of current density versus $F^{1/2}$) of the same dark current-voltage characteristics in PNECM film

Table 1 Poole-Frenkel constant β_{PF} observed for PNECM film (thickness 32 μm)

Film temperature (K)	β_{PF} (eV m ^{1/2} V ^{-1/2})	
	Observed	Calculated
300	5.45×10^{-5}	4.39×10^{-5}
309	5.34×10^{-5}	

According to PF formalism¹³:

$$\sigma_{PF} = \sigma_0 \exp(\beta_{PF} F^{1/2} / kT)$$

where $\beta_{PF} = (e^3 / \pi \epsilon \epsilon_0)^{1/2}$, σ_0 is the low field conductivity and F is the applied field. From the PF constant¹⁴ the relative dielectric constant was evaluated as 2.2. The approximate coincidence of this value with the measured value determined by means of a capacitance bridge (2.9) as indicated below supports the idea that the conduction process in PNECM is controlled by the PF mechanism.

Dependence of photocurrent on applied voltage at two different temperatures and at 120 mW cm⁻² is illustrated in Figure 5. The photocurrent at low voltage is 10 times the dark current, while at high voltage it is about 60–70 times the dark current. The nature of the graph is almost similar to that for dark current-voltage except only that the optical detrapping occurs at above 150 V instead of at 200 V (in the dark). Thus light has a greater effect on the current, and SCLC may increase markedly in the presence of light. The photocurrent increases linearly below 150 V, and then starts to increase superlinearly

above 150 V. Thus, the number of photocarriers increases with increasing applied voltage because the carriers which escape from recombination centres increase with increasing applied voltage due to the lowering of the potential barrier.

Dielectric constant and dielectric loss

The dielectric constant (2.9) and dielectric loss (4.6×10^{-6}) parameters at room temperature are independent of frequency range between 50 Hz–10 kHz which is consistent with the non-polarity of PNECM.

The dielectric constant and dielectric loss gradually increases from 2.9–4.15 and 4.6×10^{-6} to 7.2×10^{-6} , respectively, with temperature (300–344 K) at 1 kHz which may be caused by electronic and ionic polarizability.

Photocurrent kinetics

The growth and decay behaviour of the photocurrent for a PNECM film with different applied voltage at room temperature is shown in Figure 7. The intensity of illumination was 120 mW cm⁻². Clearly as the voltage increases the photoconductivity of PNECM increases and the growth and decay time of the photoconductivity are almost the same.

Photocurrent-intensity variation

Photocurrent (I_p)-intensity (I) variation of PNECM film has been investigated for different applied voltage. Photocurrent plotted against I on log-log scale at different applied voltage as shown in Figure 8 is linear. At low intensity I_p varies with I as $I^{0.89}$ whereas at high I , $I_p \propto I^{0.123}$. Thus at low I , I_p is determined by the carrier

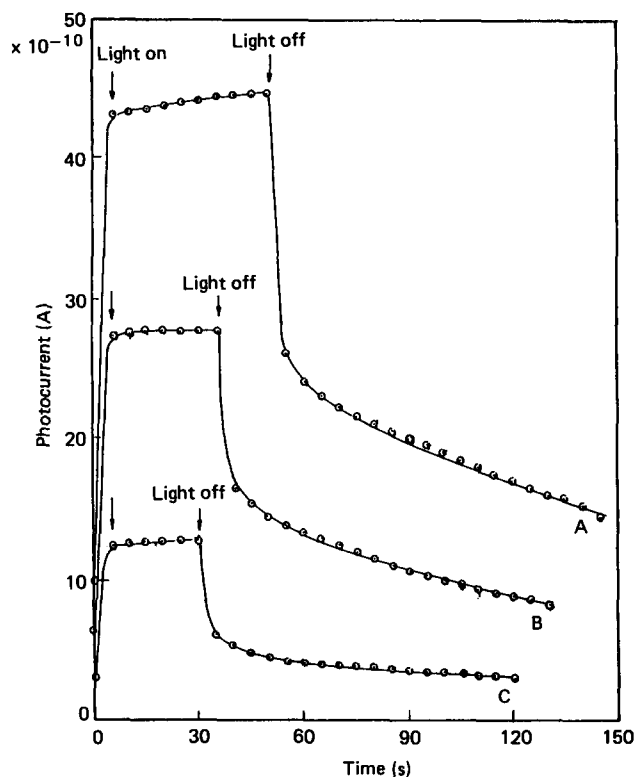


Figure 7 Growth and decay of photocurrent for different applied voltages (A, 300; B, 200; C, 100 V) and at a fixed intensity of illumination 120 mW cm⁻²

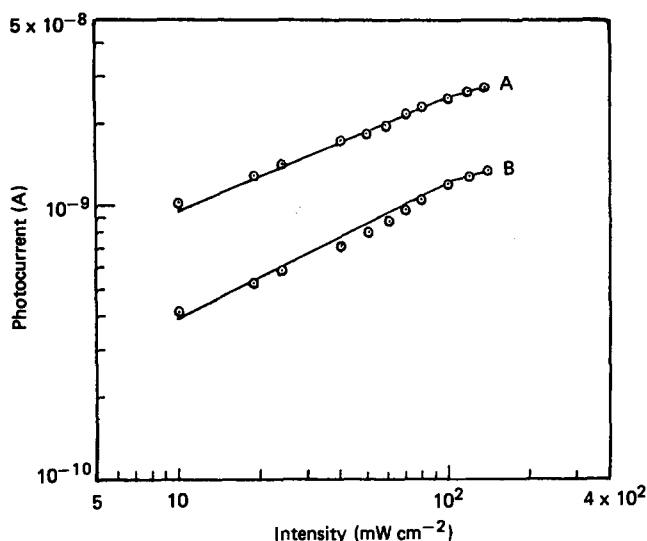


Figure 8 Photocurrent versus light intensity in PNECM film at two different applied voltages (A, 200; B, 100 V) and at room temperature (300 K)

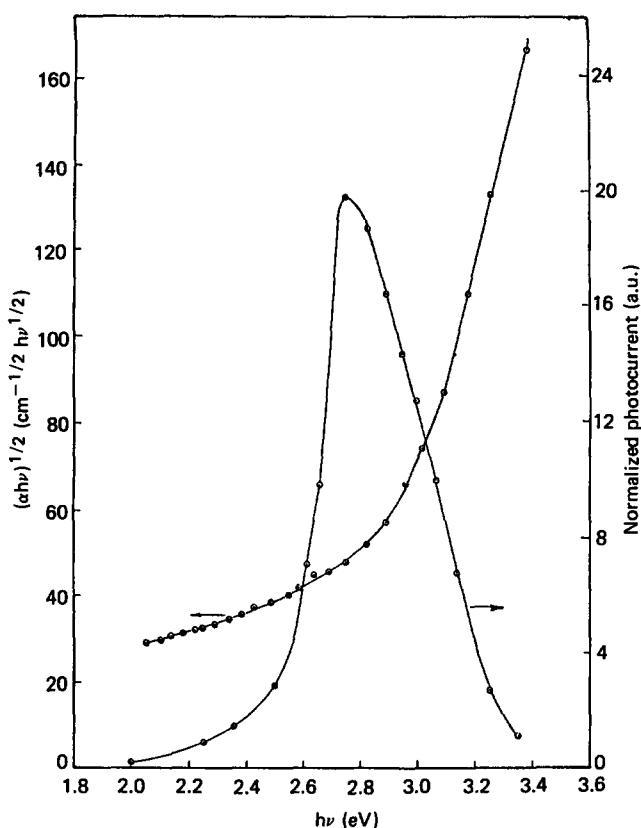


Figure 9 Square root of the product of optical absorption coefficient and photon energy versus photon energy and normalized photocurrent versus photon energy in PNECM (film thickness 32 μm) at room temperature (300 K)

generation rate, whereas at high I bimolecular recombination may play a major role in determining the full carrier yield.

Spectral properties

The variation of the optical density of PNECM film with wavelength has been measured with a Carry 17-D spectrophotometer. From the data the absorption coefficient (α) for the sample at various photon energies

($h\nu$) has been evaluated. A plot of $(\alpha h\nu)^{1/2}$ versus $h\nu$ is shown in Figure 9.

The spectral dependence of I_p of PNECM film is also shown in Figure 9. A pronounced maximum in the plot is found at 2.75 eV. The graph shown in Figure 9 can be interpreted as the photoionization of defect states in the band gap. The sample has a penetration depth for active radiation that already falls in the region of the absorption edge, and thus I_p falls at the absorption edge as the volume of the irradiated sample decreases¹⁶.

Since I_p increases linearly in a low electric field, and then starts to increase remarkably in the higher electric field region, the number of photocarriers increases with increasing field strength, because the carriers which escape from the geminate recombination centre increase with increasing field strength. Therefore, it is quite usual that I_p is superlinear at high fields as observed. This field dependence may be explained in many cases by the Onsager¹⁶ relation.

On prolonged heating in air a light green coloured polymer has been obtained by slow oxidation. It has no photoconductivity. The probable reason is that quinonoid type of structures formed on oxidation of the monomer moiety possibly act as deep traps for electrons and thus the n-type photoconducting polymer loses its photoconductivity.

Thermally stimulated current

A t.s.c. spectrum is shown in Figure 10. This first t.s.c. spectrum includes the currents caused by the release of trapped carrier as well as by the polarization of dipoles. In order to distinguish between them, the bias voltage is removed from the sample near the softening point, and dipoles relax back to their previous random positions. The sample is recooled to low temperature and reheated at the same rate after the application of the same bias voltage. On the cycle, as there has been no irradiation and thus no trapped carriers, the t.s.c. spectrum excludes the contribution of trapped carriers. Therefore, the difference

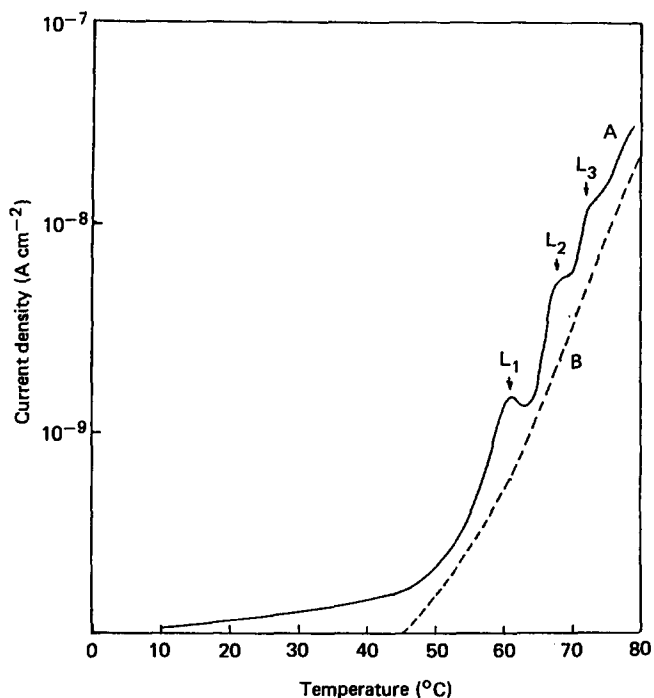


Figure 10 First (A) and second (B) t.s.c. spectra for PNECM film

Table 2 T.s.c. peaks for PNECM film (thickness 32 μm)

Peaks	Peaks from carrier detrapping ($^{\circ}\text{C}$)
L ₁	61.5
L ₂	68.0
L ₃	72.0

between the first and second t.s.c. spectra is due to the release of trapped carriers. Thus, the contribution of dipoles to t.s.c. is negligibly small for PNECM because it does not contain any relaxation phenomena due to random orientation of monomer moieties. Similar observation was noticed by Suzuoki *et al.*⁶ in polyethylene. The major t.s.c. peaks due to trapped carriers are summarized in Table 2.

In conclusion, it may be mentioned that this polymer based on a carbazole moiety can display promising photoconductivity as poly(*N*-vinyl carbazole).

REFERENCES

- 1 Pramanik, P., Mukherjee, D. and Choudhury, T. K. *Ind. J. Chem.* 1984, **23A**(10), 839
- 2 Akhter, M. A., Pramanik, P. and Biswas, M. *J. Polym. Sci., Polym. Phys. Edn. (B)* 1987, **25**, 339
- 3 Perlman, M. M. *J. Electrochem. Soc.* 1972, **119**, 892
- 4 Perlman, M. M. and Unger, S. *J. Appl. Phys.* 1972, **5**, 2115
- 5 Blake, A. E., Charlesby, A. and Randle, K. J. *J. Appl. Phys.* 1974, **7**, 759
- 6 Suzuoki, Y., Nizutani, T. and Ieda, M. *Jap. J. Appl. Phys.* 1976, **15**(5), 929
- 7 Nishitani, T., Yoshino, K. and Inuishi, Y. *Jap. J. Appl. Phys.* 1975, **14**, 721
- 8 Kang, E. T., Ehrlich, P., Bhatt, A. P. and Anderson, W. A. *Macromolecules* 1984, **17**, 1020
- 9 Yun, M. S., Ozaki, M., Yoshino, K. and Inuishi, Y. *Jap. J. Appl. Phys.* 1983, **22**(12), 1910
- 10 Compos, M. *Mol. Cryst. Liq. Cryst.* 1972, **18**, 105
- 11 Helfrich, W. and Mark, P. Z. *Physik* 1962a, **168**, 495
- 12 Helfrich, W. and Mark, P. Z. *Physik* 1962b, **166**, 370
- 13 Simmons, J. G. *Phys. Rev.* 1967, **155**, 657
- 14 Okamoto, K., Kusabayashi, S., Yokoyama, M., Kato, K. and Mikawa, H. *Soc. Photogr. Sci. Eng., 2nd Int. Conf. on Electrophotog.*, Washington DC, 1974, 81
- 15 Hauschildt, D., Fuhs, W. and Hesse, H. J. *Phys. Stat. Sol.* 1979, **B91**, 447
- 16 Onsager, L. *Phys. Rev.* 1938, **58**, 554